

# EARTH'S GLOBAL ENERGY BUDGET

BY KEVIN E. TRENBERTH, JOHN T. FASULLO, AND JEFFREY KIEHL

An update of the Earth's global annual mean energy budget is given in the light of new observations and analyses. Changes over time and contributions from the land and ocean domains are also detailed.

Weather and climate on Earth are determined by the amount and distribution of incoming radiation from the sun. For an equilibrium climate, OLR<sup>1</sup> necessarily balances the incoming ASR, although there is a great deal of fascinating atmosphere, ocean, and land phenomena that couple the two. Incoming radiant energy may be scattered and reflected by clouds and aerosols or absorbed in the atmosphere. The transmitted radiation is then either absorbed or reflected at the Earth's surface. Radiant solar or shortwave energy is transformed into sensible heat, latent energy (involving different water states), potential energy, and kinetic energy before being emitted as longwave radiant energy. Energy may be stored for some time, transported

in various forms, and converted among the different types, giving rise to a rich variety of weather or turbulent phenomena in the atmosphere and ocean. Moreover, the energy balance can be upset in various ways, changing the climate and associated weather.

Kiehl and Trenberth (1997, hereafter KT97) reviewed past estimates of the global mean flow of energy through the climate system and presented a new global mean energy budget based on various measurements and models. They also performed a number of radiative computations to examine the spectral features of the incoming and outgoing radiation and determined the role of clouds and various greenhouse gases in the overall radiative energy flows. At the TOA, values relied heavily on observations from the ERBE from 1985 to 1989, when the TOA values were approximately in balance. In this paper we update those estimates based on more recent observations, which include improvements in retrieval methodology and hardware, and discuss continuing sources of uncertainty.

State-of-the-art radiative models for both longwave and shortwave spectral regions were used by KT97 to partition radiant energy for both clear and cloudy skies. Surface sensible and latent heat estimates were based on other observations and analyses. During ERBE, it is now thought that the imbalance

**AFFILIATIONS:** TRENBERTH, FASULLO, AND KIEHL—National Center for Atmospheric Research,\* Boulder, Colorado

\*The National Center for Atmospheric Research is sponsored by the National Science Foundation

**CORRESPONDING AUTHOR:** Kevin E. Trenberth, National Center for Atmospheric Research; P.O. Box 3000, Boulder, CO 80307-3000

E-mail: trenbert@ucar.edu

*The abstract for this article can be found in this issue, following the table of contents.*

DOI:10.1175/2008BAMS2634.1

In final form 29 July 2008

©2009 American Meteorological Society

<sup>1</sup> A list of all acronyms is given in the appendix.

at the TOA was small (Levitus et al. 2005), and KT97 set it to zero. KT97 estimated all of the terms but adjusted the surface sensible heat estimate to ensure an overall balance at the surface. At the TOA, the imbalance in the raw ERBE estimates was adjusted to zero by making small changes to the albedo on the grounds that greatest uncertainties remained in the ASR (Trenberth 1997). In addition, adjustments were made to allow for the changes observed when one of the three ERBE satellites failed. Improvements are now possible.

KT97 was written at a time when there was a lot of concern over “anomalous cloud absorption.” This expression came from observations (Stephens and Tsay 1990; Cess et al. 1995; Ramanathan et al. 1995; Pilewskie and Valero 1995) that suggested that clouds may absorb significantly more shortwave radiation (approximately  $20\text{--}25\text{ W m}^{-2}$ ) than was accounted for in model calculations (such as the models employed by KT97). Since then both radiation observations and models have improved (e.g., Oreopoulos et al. 2003), and so too have estimates of key absorbers, such as water vapor (Kim and Ramanathan 2008). Other observations have suggested that the absorption by aerosols in KT97 were underestimated by  $2\text{--}5\text{ W m}^{-2}$  (Ramanathan et al. 2001; Kim and Ramanathan 2008) so that this amount is lost from the surface.

Major recent advances in understanding the energy budget have been provided by satellite data and globally gridded reanalyses (e.g., Trenberth et al. 2001; Trenberth and Stepaniak 2003a,b, 2004). Trenberth et al. (2001) performed comprehensive estimates of the atmospheric energy budget based on two first-generation atmospheric reanalyses and several surface flux estimates, and made crude estimates of uncertainty. The atmospheric energy budget has been documented in some detail for the annual cycle (Trenberth and Stepaniak 2003a, 2004) and for ENSO and interannual variability (Trenberth et al. 2002; Trenberth and Stepaniak 2003a). The radiative aspects have been explored in several studies by Zhang et al. (2004, 2006, 2007) based on ISCCP cloud data and other data in an advanced radiative code. In addition, estimates of surface radiation budgets have been given by Gupta et al. (1999) and used by Smith et al. (2002) and Wilber et al. (2006). These are based on earlier ISCCP data. Wild et al. (2006) evaluated climate models for solar fluxes and note that large uncertainties still exist, even for clear-sky fluxes, although they also note recent improvements in many models.

Many new measurements have now been made from space, notably from CERES instruments on sev-

eral platforms (Wielicki et al. 1996, 2006). Moreover, there are a number of new estimates of the atmospheric energy budget possible from new atmospheric reanalyses, to the extent that the results from the assimilating model can be believed. Several analyses of ocean heat content also help constrain the problem, and together these provide a more holistic view of the global heat balance. Accordingly, Fasullo and Trenberth (2008a) provide an assessment of the global energy budgets at TOA and the surface, for the global atmosphere, and ocean and land domains based on a synthesis of satellite retrievals, reanalysis fields, a land surface simulation, and ocean temperature estimates. They constrain the TOA budget to match estimates of the global imbalance during recent periods of satellite coverage associated with changes in atmospheric composition and climate. There is an annual mean transport of energy by the atmosphere from ocean to land regions of  $2.2 \pm 0.1\text{ PW}$  ( $1\text{ PW} = 10^{15}\text{ W}$ ) primarily in the northern winter when the transport exceeds  $5\text{ PW}$ . Fasullo and Trenberth (2008b) go on to evaluate the meridional structure and transports of energy in the atmosphere, ocean, and land for the mean and annual cycle zonal averages over the ocean, land, and global domains. Trenberth and Fasullo (2008) delve into the ocean heat budget in considerable detail and provide an observationally based estimate of energy divergence and a comprehensive assessment of uncertainty.

By separately analyzing the land and ocean domains, Fasullo and Trenberth (2008a) discovered a problem in the earlier adjustment made to ERBE data when NOAA-9 failed, and found it desirable to homogenize the record separately over ocean and land rather than simply globally. The result is a revised and slightly larger value for the global OLR than in KT97. However, even bigger changes arise from using CERES data that presumably reflect the improved accuracy of CERES retrievals and its advances in retrieval methodology, including its exploitation of MODIS retrievals for scene identification.

Therefore, in this paper, we build on the results of Fasullo and Trenberth (2008a,b) that provided the overall energy balance for the recent CERES period from March 2000 to May 2004 to update other parts of the energy cycle in the KT97 figure of flows through the atmosphere. To help understand sources of errors and discrepancies among various estimates, we also break down the budgets into land and ocean domains, and we separately examine the ERBE and CERES periods to provide an assessment related to the changes in technology and effects of climate change. We also better incorporate effects of

the spatial structure and annual and diurnal cycles, which rectify onto the global mean values.

**DATASETS.** Satellite measurements provide the “best estimate” of TOA terms. Satellite retrievals from the ERBE and the CERES (Wielicki et al. 1996) datasets are used (see Fasullo and Trenberth 2008a for details). ERBE estimates are based on observations from three satellites [ERBS, NOAA-9 (the scanner failed in January 1987), and NOAA-10] for February 1985–April 1989. The CERES instruments used here (FM1 and FM2) are flown aboard the *Terra* satellite, which has a morning equatorial crossing time and was launched in December 1999 with data extending to May 2004 (cutoff for this study). We compile monthly means for the available data period and use those to compute an annual mean.

There is a TOA imbalance of  $6.4 \text{ W m}^{-2}$  from CERES data and this is outside of the realm of current estimates of global imbalances (Willis et al. 2004; Hansen et al. 2005; Huang 2006) that are expected from observed increases in carbon dioxide and other greenhouse gases in the atmosphere. The TOA energy imbalance can probably be most accurately determined from climate models and is estimated to be  $0.85 \pm 0.15 \text{ W m}^{-2}$  by Hansen et al. (2005) and is supported by estimated recent changes in ocean heat content (Willis et al. 2004; Hansen et al. 2005). A comprehensive error analysis of the CERES mean budget (Wielicki et al. 2006) is used in Fasullo and Trenberth (2008a) to guide adjustments of the CERES TOA fluxes so as to match the estimated global imbalance. CERES data are from the SRBAVG (edition 2D rev 1) data product. An upper error bound on the longwave adjustment is  $1.5 \text{ W m}^{-2}$ , and OLR was therefore increased uniformly by this amount in constructing a best estimate. We also apply a uniform scaling to albedo such that the global mean increase from 0.286 to 0.298 rather than scaling ASR directly, as per Trenberth (1997), to address the remaining error. Thus, the net TOA imbalance is reduced to an acceptable but imposed  $0.9 \text{ W m}^{-2}$  (about 0.5 PW). Even with this increase, the global mean albedo is significantly smaller than for KT97 based on ERBE [0.298 versus 0.313; see Fasullo and Trenberth (2008a) for details].

The most comprehensive estimates of global atmospheric temperature and moisture fields are available from reanalyses of the NRA (Kalnay et al. 1996) and the second-generation ERA-40 (Uppala et al. 2005) and recent JRA (Onogi et al. 2007). These reanalyses provide estimates of radiative fluxes at the TOA and surface as well as surface fluxes, and these will be examined here.

A new estimate of the global hydrological cycle is given in Trenberth et al. (2007a). In particular, various estimates of precipitation are compared and evaluated for the land, ocean, and global domains for the annual and monthly means with error bars assigned. The main global datasets available for precipitation that merge in situ with satellite-based estimates of several kinds, and therefore include ocean coverage, are the GPCP (Adler et al. 2003) and CMAP (Xie and Arkin 1997). Comparisons of these datasets and others (e.g., Yin et al. 2004) reveal large discrepancies over the ocean; and over the tropical oceans, mean amounts in CMAP are greater than GPCP by 10%–15%. GPCP is biased low by 16% at small tropical atolls (Adler et al. 2003). However, GPCP are considered the more reliable, especially for time series, and use is made of data from 1988 to 2004. The net atmospheric moisture transport from ocean to land, and the corresponding return flow in rivers and runoff was estimated to be  $40 \pm 1 \times 10^3 \text{ km}^3 \text{ yr}^{-1}$  (Dai and Trenberth 2002; Trenberth et al. 2007a), which is equivalent to  $3.2 \pm 0.1 \text{ PW}$  of latent energy (error bars are two standard deviations). We also use estimates of the surface heat balance from a comprehensive land surface model, namely, the CLM3, forced with observation-based precipitation, temperature, and other atmospheric forcing to simulate historical land surface conditions (Qian et al. 2006). The CLM3 simulations provide complementary information for evapotranspiration and the net surface energy flux over land.

Other estimates of radiative and surface fluxes have been derived using satellite data, including those made by the ISCCP (Rossow and Duenas 2004; Zhang et al. 2004) and CERES (Loeb et al. 2000, 2007, 2009; Wielicki et al. 2006) groups. Zhang et al. (2004) produce the ISCCP-FD version of radiative fluxes based upon ISCCP cloud data and other data in an advanced radiative code. This has been produced in 3-h steps globally on a 280-km grid from July 1983 onward. They estimate, based on comparisons with ERBE, limited CERES, and some surface data, that the errors are of the order of  $5\text{--}10 \text{ W m}^{-2}$  at TOA and  $10\text{--}15 \text{ W m}^{-2}$  at the surface. For their dataset the net radiation at the TOA is  $+4.7 \text{ W m}^{-2}$  for the ERBE period. Kim and Ramanathan (2008) provide updated estimates of the solar radiation budget by making use of many space-based measurements in a model with new treatment of water vapor absorption and aerosols for 2000–02. The results were validated using surface observations but were not constrained by requirements for a balanced budget. Very recently, Loeb et al. (2009), stimulated by the Fasullo and Trenberth (2008a,b) results, have provided a CERES

team view of the closure for the TOA radiation budget. The TOA imbalance in the original CERES products is reduced by making largest changes to account for the uncertainties in the CERES instrument absolute calibration. They also use a lower value for solar irradiance taken from the recent TIM observations (Kopp et al. 2005).

Several atlases exist of surface flux data, but they are fraught with global biases of several tens of watts per meter squared in unconstrained VOS observation-based products (Grist and Josey 2003) that show up, especially when net surface flux fields are globally averaged. These include some based on bulk flux formulas and in situ measurements, such as the Southampton Oceanographic Centre (SOC) from Grist and Josey (2003), WHOI (Yu et al. 2004; Yu and Weller 2007), and satellite data, such as the HOAPS data, now available as HOAPS version 3 (Bentamy et al. 2003; Schlosser and Houser 2007). The latter find that space-based precipitation  $P$  and evaporation  $E$  estimates are globally out of balance by about an unphysical 5%. There are also spurious variations over time as new satellites and instruments become part of the observing system.

Zhang et al. (2006) find uncertainties in ISCCP-FD surface radiative fluxes of 10–15  $\text{W m}^{-2}$  that arise from uncertainties in both near-surface temperatures and tropospheric humidity. Zhang et al. (2007) computed surface ocean energy budgets in more detail by combining radiative results from ISCCP-FD with three

surface turbulent flux estimates, from HOAPS-2, NCEP reanalyses, and WHOI (Yu et al. 2004). On average, the oceans surface energy flux was +21  $\text{W m}^{-2}$  (downward), indicating that major biases are present. They suggest that the net surface radiative heating may be slightly too large (Zhang et al. 2004), but also that latent heat flux variations are too large.

There are spurious trends in the ISCCP data (e.g., Dai et al. 2006) and evidence of discontinuities at times of satellite transitions. For instance, Zhang et al. (2007) report earlier excellent agreement of ISCCP-FD with the ERBS series of measurements in the tropics, including the decadal variability. However, the ERBS data have been reprocessed (Wong et al. 2006), and no significant trend now exists in the OLR, suggesting that the previous agreement was fortuitous (Trenberth et al. 2007b).

Estimates of the implied ocean heat transport from the NRA, indirect residual techniques, and some coupled models are in reasonable agreement with hydrographic observations (Trenberth and Caron 2001; Grist and Josey 2003; Trenberth and Fasullo 2008). However, the hydrographic observations also contain significant uncertainties resulting from both large natural variability and assumptions associated with their indirect estimation of the heat transport, and these must be recognized when using them to evaluate the various flux products. Nevertheless, the ocean heat transport implied by the surface fluxes provides a useful metric and constraint for evaluating products.

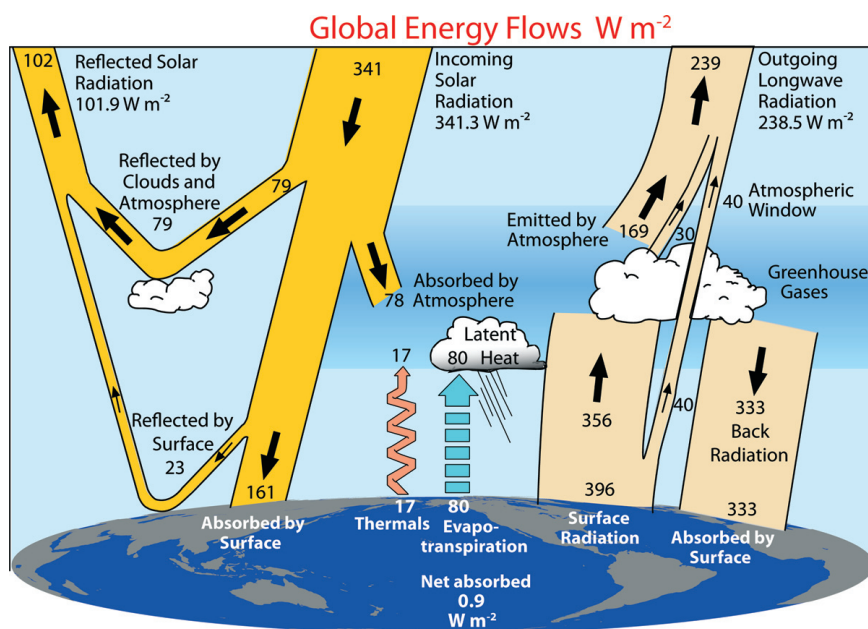


**FIG. 1. The global annual mean Earth's energy budget for the Mar 2000 to May 2004 period ( $\text{W m}^{-2}$ ). The broad arrows indicate the schematic flow of energy in proportion to their importance.**

## THE GLOBAL MEAN ENERGY BUDGET.

The results are given here in Table 1 for the ERBE period, Table 2 for the CERES period, and Fig. 1 also for the CERES period. The tables present results from several sources and for land, ocean, and global domains. Slight differences exist in the land and ocean masks, so that the global value may consist of slightly different weights for each component.

*ERBE period results.* For the ERBE period, Table 1 presents results from KT97 for comparison with those



of ISCCP-FD (calculated on its native equal-area grid), and the three reanalyses NRA, ERA-40, and JRA (which have been regridded to a common T63 grid), with two major parts to the table for the TOA (Table 1a) and surface (Table 1b). Estimates of ocean heat content during ERBE (Levitus et al. 2005) suggest that there was little or no change and this applies then to the global net (Fasullo and Trenberth 2008a). Accordingly, the reanalyses are seriously out of balance by order  $10 \text{ W m}^{-2}$  and all produce net cooling. The NRA has a known bias in much too high surface albedo over the oceans (Kalnay et al. 1996) that is especially evident in the ocean TOA values (Table 1) and cloud distribution and properties are responsible for substantial errors in both ASR and OLR (Bony et al. 1997; Weare 1997; Trenberth et al. 2001). In ERA-40 OLR is too large by  $5\text{--}30 \text{ W m}^{-2}$  almost everywhere, except in regions of deep convection,

and the global bias was  $9.4 \text{ W m}^{-2}$  in January 1989 (Trenberth and Smith 2008a). Problems with clouds also mainly account for the biases in JRA (Trenberth and Smith 2008b).

At the surface, values are provided for the latent and sensible heat fluxes (LH and SH) as well as the radiative terms, and the net overall is the sum of the solar downward, the net LW upward, and the LH and SH fluxes (upward). The downward land flux associated with global warming (that accounts for melting land ice, etc.) is estimated to be less than about  $0.01 \text{ PW}$ , or  $0.07 \text{ W m}^{-2}$ . Thus, in the reanalyses (Table 1b), the net downward flux into the ground is too large to be plausible. Over oceans (Table 1b), to the extent that the net TOA globally is approximately zero for the ERBE period, the ocean warming should also be small and so the net surface flux over ocean is largely a measure of the errors. From Trenberth

## SPATIAL AND TEMPORAL SAMPLING

**A**lthough we are primarily interested in the global mean energy budget in this paper, it is desirable to assess and account for rectification effects. For example, in KT97, we used a single column model constrained by observations, to represent the average fluxes in the atmosphere. We compared results at TOA with those from the NCAR CCM3 and found good agreement, so that the spatial structure was accounted for. At the surface, the outgoing radiation was computed for blackbody emission at  $15^\circ\text{C}$  using the Stefan–Boltzmann law

$$R = \epsilon \sigma T^4, \quad (1)$$

where the emissivity  $\epsilon$  was set to 1.

If we define a global mean as  $T_g$ , then  $T = T_g + T'$ , where the  $T'$  refers to departures from the global mean in either time or space. Therefore,  $T^4 = T_g^4(1 + T'/T_g)^4$ . We expand the bracket and take the global mean, so that the  $T'$  and  $T^3$  terms vanish, and then

$$T^4 = T_g^4(1 + 6[T'/T_g]^2 + (T'/T_g)^4). \quad (2)$$

The ratio  $T'/T_g$  is relatively small. For 1961–90, Jones et al. (1999) estimate that  $T_g$  is  $287.0 \text{ K}$ , and the largest fluctuations in time correspond to the annual cycle of  $15.9^\circ\text{C}$  in July to  $12.2^\circ\text{C}$  in January, or  $1.3\%$ . Accordingly, the extra terms are negligible for temporal variations owing to the compensation from the different hemispheres in day versus night or winter versus summer. However, spatially time-averaged temperatures can vary from  $-40^\circ\text{C}$  in polar regions to  $30^\circ\text{C}$  in the tropical deserts. With a  $28.7\text{-K}$  variation (10% of global mean) the last term in (2) is negligible, but the second term becomes a nontrivial 6% increase.

To compute these effects more exactly, we have taken the surface skin temperature from the NRA at T62 resolution and 6-h sampling and computed the correct global mean surface radiation from (1) as  $396.4 \text{ W m}^{-2}$ . If we instead take the daily average values, thereby removing the diurnal cycle effects, the value drops to  $396.1 \text{ W m}^{-2}$ , or a small negative bias. However, large changes occur if we first take the global mean temperature. In that case the answer is the same for 6-hourly, daily, or climatological means at  $389.2 \text{ W m}^{-2}$ . Hence, the lack of resolution of the spatial structure leads to a low bias of about  $7.2 \text{ W m}^{-2}$ . Indeed, when we compare the surface upward radiation from reanalyses that resolve the full spatial structure the values range from  $393.4$  to  $396.0 \text{ W m}^{-2}$ .

The surface emissivity is not unity, except perhaps in snow and ice regions, and it tends to be lowest in sand and desert regions, thereby slightly offsetting effects of the high temperatures on LW upwelling radiation. It also varies with spectral band (see Chédin et al. 2004, for discussion). Wilber et al. (1999) estimate the broadband water emissivity as  $0.9907$  and compute emissions for their best-estimated surface emissivity versus unity. Differences are up to  $6 \text{ W m}^{-2}$  in deserts, and can exceed  $1.5 \text{ W m}^{-2}$  in barren areas and shrublands.

Similar rectification effects may occur for the back radiation to the surface, so that for KT97 the errors tend to offset, but the surface radiation exchanges should be enhanced by about  $6 \text{ W m}^{-2}$ .

**TABLE 1a. TOA annual mean radiation budget quantities for the ERBE period of Feb 1985 to Apr 1989 for global, global land, and global ocean. The downward solar (Solar In), reflected solar (Solar reflected), and net (NET down) radiation are given with the ASR and OLR ( $\text{W m}^{-2}$ ), and albedo is given in percent. The ERBE FT08 is from Fasullo and Trenberth (2008a); and other values are from KT97, ISCCP-FD, and the three reanalyses: NRA, ERA-40, and JRA.**

Global	Solar In	Solar reflected	Albedo (%)	ASR	OLR	NET down
KT97	341.8	107	31	235	235	0.0
ERBE FT08	341.3	106.9	31.3	234.4	234.4	0.0
ISCCP-FD	341.8	105.9	31.0	235.8	233.3	2.5
NRA	341.9	115.6	33.8	226.3	237.4	-11.1
ERA-40	342.5	106.0	31.0	236.5	245.0	-8.5
JRA	339.1	95.2	28.1	234.8	253.9	-10.1
<b>Land</b>						
ERBE FT08	330.1	118.0	35.8	212.1	228.7	-16.6
ISCCP-FD	330.9	113.8	34.4	217.1	228.0	-10.9
NRA	330.7	116.4	35.2	214.4	232.9	-18.5
ERA-40	330.3	110.0	33.3	220.2	239.0	-18.8
JRA	328.2	101.1	30.8	227.1	249.7	-22.6
<b>Ocean</b>						
ERBE FT08	345.3	102.9	29.8	242.2	236.4	6.0
ISCCP-FD	345.9	102.9	29.7	243.2	235.2	8.0
NRA	346.0	115.4	33.3	230.6	239.0	-8.4
ERA-40	346.9	104.6	30.2	242.3	247.2	-4.9
JRA	343.0	93.1	27.1	249.9	255.4	-5.5

et al. (2007a), the net evaporation for 1988–2004 over ocean and land are 89 and 41  $\text{W m}^{-2}$ , respectively. Accordingly, the evaporative LH fluxes are too high over land for NRA and over oceans for ERA-40, JRA, and HOAPS by order of 10  $\text{W m}^{-2}$ , while the values from WHOI and NRA over oceans are reasonably close. Hence, for ERA-40, NRA, and ISCCP-FD, the implication is an error of up to 20  $\text{W m}^{-2}$  at the surface in the other terms, and we believe this is most likely in the net downward LW radiation, as discussed later. Unlike the other reanalyses, JRA has a negative (upward) net surface flux over the oceans that comes from much too large LH, SH, and net LW fluxes upward.

The chronic problems in correctly emulating the distribution and radiative properties of clouds realistically in the reanalyses preclude those as useful guides for our purpose of determining a new global mean value. Accordingly, the most realistic published computations to date appear to be those of Zhang et al. (2004) in the ISCCP-FD dataset in which observed clouds were used every 3 h, at least for the solar components where the TOA view of clouds is most pertinent. For the surface LW radiation, however, the

results are highly dependent on the cloud-base height and radiative properties that are not well determined by space-based measurements. Thus, the downwelling LW flux exists as one of the principle uncertainties in the global surface energy budget.

**CERES period results.** For the CERES period, March 2000–May 2004, Table 2 presents similar results except ERA-40 data are not available and we have included our present best estimate. At the TOA our values are determined from the CERES values as adjusted by Fasullo and Trenberth (2008a). As noted in the “Datasets” section, the TOA energy imbalance can probably be most accurately determined from climate models and Fasullo and Trenberth (2008a) reduced the imbalance to be 0.9  $\text{W m}^{-2}$ , where the error bars are  $\pm 0.15 \text{ W m}^{-2}$ .

For the surface we initially made estimates of the various terms, but encountered an imbalance of order 20  $\text{W m}^{-2}$ , which led us to reexamine the assumptions. At first, we computed the solar radiation absorbed in the atmosphere, the surface-reflected radiation, and the net solar radiation absorbed at

**TABLE 1b. Surface components of the annual mean energy budget for the globe, global land, and global ocean, except for atmospheric solar radiation absorbed (Solar absorb, left column), for the ERBE period of Feb 1985 to Apr 1989 ( $\text{W m}^{-2}$ ). Included are the solar absorbed at the surface (Solar down), reflected solar at the surface (Solar reflect), surface latent heat from evaporation (LH evaporation), sensible heat (SH), LW radiation up at the surface (Radiation up), LW downward radiation to the surface (Back radiation), net LW (Net LW), and net energy absorbed at the surface (NET down). HOAPS version 3 covers  $80^{\circ}\text{S}$ – $80^{\circ}\text{N}$  and is for 1988 to 2005. The ISCCP-FD is combined with HOAPS to provide a NET value.**

<b>Global</b>	Solar absorb	Solar down	Solar reflect	LH evaporation	SH	Radiation up	Back radiation	Net LW	NET down
KT97	67	168	24	78	24	390	324	66	0
ISCCP-FD	70.9	164.9	24.0	-	-	395.9	344.8	51.1	-
NRA	64.4	161.9	45.2	80.2	15.3	395.5	334.1	61.5	4.9
ERA-40	80.7	155.8	23.1	82.3	15.3	394.8	340.3	54.4	3.8
JRA	75.0	168.9	25.6	85.1	18.8	395.6	324.3	71.3	-6.3
<b>Land</b>									
ISCCP-FD	69.9	147.2	42.9	-	-	377.8	318.7	57.5	-
NRA	59.1	155.2	68.9	52.0	27.1	369.7	295.9	73.8	2.3
ERA-40	86.0	134.3	42.9	40.9	25.8	370.3	304.9	65.3	2.3
JRA	72.2	154.9	51.5	39.5	27.3	372.7	286.7	86.0	2.1
<b>Ocean</b>									
ISCCP-FD	71.4	171.5	17.0	-	-	402.7	354.5	48.2	10.4
NRA	66.3	164.3	36.7	90.3	11.0	404.9	347.9	57.0	6.0
ERA-40	78.8	163.5	15.9	97.3	11.5	403.6	353.1	50.5	4.2
JRA	76.0	173.9	16.2	101.5	15.8	403.9	337.9	66.0	-9.4
WHOI	-	-	-	91.2	9.5	-	-	-	-
HOAPS	-	-	-	98.9	14.0	-	-	54.1	-

the surface by taking the ISCCP-FD values adjusted by the ratio of the CERES to ISCCP-FD ASR values. This results in the value given in Table 2b for the surface-reflected component. For the absorbed atmospheric solar radiation, the result was  $71.6 \text{ W m}^{-2}$  and the solar radiation absorbed at the surface was  $167.7 \text{ W m}^{-2}$ . Wild and Roeckner (2006) note the likely importance of improved aerosol climatologies. Moreover, Kim and Ramanathan (2008) find that updated spectroscopic parameters and continuum absorption for water vapor increases the absorption by  $4\text{--}6 \text{ W m}^{-2}$  relative to these values. In addition, water vapor concentrations have increased throughout the troposphere at about  $1.2\%$  decade $^{-1}$  since the ERBE period (Trenberth et al. 2005, 2007b). They also note the increase from absorption by aerosols relative to the values of KT97, who placed the net atmospheric absorption at  $67 \text{ W m}^{-2}$ . Accordingly, their total absorbed solar radiation is  $78.2 \text{ W m}^{-2}$  (where we have adjusted for their different total solar irradiance and albedo), and we adopt this here. Accordingly, the net absorbed at the surface is reduced to  $161.2 \text{ W m}^{-2}$ .

Global precipitation should equal global evaporation for a long-term average, and estimates are likely more reliable of the former. However, there is considerable uncertainty in precipitation over both the oceans and land (Trenberth et al. 2007b; Schlosser and Houser 2007). The latter is mainly due to wind effects, undercatch, and sampling, while the former is due to shortcomings in remote sensing. GPCP values are considered most reliable (Trenberth et al. 2007b), and for 2000–04 the global mean is  $2.63 \text{ mm day}^{-1}$ , which is equivalent to  $76.2 \text{ W m}^{-2}$  latent heat flux. For the same period, global CMAP values are similar at  $2.66 \text{ mm day}^{-1}$ , but values are smaller than GPCP from  $30^{\circ}$  to  $90^{\circ}$  latitude and larger from  $30^{\circ}\text{S}$  to  $30^{\circ}\text{N}$ . If the CMAP extratropical values are mixed with GPCP tropical values, and vice versa, the global result ranges from  $2.5$  to  $2.8 \text{ mm day}^{-1}$ . In addition, new results from CloudSat (e.g., Stephens and Haynes 2007) may help improve measurements, with prospects mainly for increases in precipitation owing to undersampling low, warm clouds. Consequently, the GPCP values are considered to likely be low. In

**TABLE 2a. TOA annual mean radiation budget quantities for the CERES period of Mar 2000 to May 2004 for global, global land, and global ocean. The downward solar (Solar in), reflected solar (Solar reflected), and net (NET down) radiation are given with the ASR and OLR ( $\text{W m}^{-2}$ ), and albedo is given in percent. The values are from ISCCP-FD, the reanalyses NRA and JRA, and this paper.**

Global	Solar in	Solar reflected	Albedo (%)	ASR	OLR	NET down
ISCCP-FD	341.7	105.2	30.8	236.5	235.6	0.9
NRA	341.8	117.0	34.2	224.5	237.8	-13.0
JRA	339.1	94.6	27.9	244.5	253.6	-9.1
This paper	341.3	101.9	29.8	239.4	238.5	0.9
<b>Land</b>						
ISCCP-FD	330.9	111.6	33.7	219.3	231.3	-12.0
NRA	330.6	116.4	35.2	214.2	234.7	-20.5
JRA	328.3	100.6	30.6	227.7	250.8	-23.1
This paper	330.2	113.4	34.4	216.8	232.4	-15.6
<b>Ocean</b>						
ISCCP-FD	345.7	102.9	29.8	242.8	237.2	5.6
NRA	345.9	117.3	33.9	228.7	238.9	-10.2
JRA	343.0	92.5	27.0	250.5	254.7	-4.2
This paper	345.4	97.8	28.3	247.7	240.8	6.9

**TABLE 2b. Surface components of the annual mean energy budget for the globe, global land, and global ocean, except for atmospheric solar radiation absorbed (Solar absorb, left column), for the CERES period of Mar 2000 to May 2004 ( $\text{W m}^{-2}$ ). Included are the solar absorbed at the surface (Solar down), reflected solar at the surface (Solar reflected), surface latent heat from evaporation (LH evaporation), sensible heat (SH), LW radiation up at the surface (Radiation up), LW downward radiation to the surface (Back radiation), net LW (Net LW), and net energy absorbed at the surface (NET down). HOAPS version 3 covers  $80^{\circ}\text{S}$ – $80^{\circ}\text{N}$  and is for 1988 to 2005. The values are from ISCCP-FD, NRA, JRA, and this paper. For the ocean, the ISCCP-FD is combined with HOAPS to provide a NET value.**

Global	Solar absorbed	Net solar	Solar reflected	LH evaporation	SH	Radiation up	Back radiation	Net LW	NET down
ISCCP-FD	70.8	165.7	22.8	-	-	393.9	345.4	48.5	-
NRA	64.4	160.4	45.2	83.1	15.6	396.9	336.5	60.4	1.3
JRA	74.7	169.8	25.6	90.2	19.4	396.9	324.1	72.8	-12.6
This paper	78.2	161.2	23.1	80.0	17	396	333	63	0.9
<b>Land</b>									
ISCCP-FD	70.6	148.7	40.1	-	-	381.2	327.6	53.6	-
NRA	59.1	155.1	70.3	50.2	26.3	371.0	296.8	74.1	4.5
JRA	71.9	155.8	51.6	39.4	27.4	374.4	287.4	87.0	2.0
This paper	78.0	145.1	39.6	38.5	27	383.2	303.6	79.6	0.0
<b>Ocean</b>									
ISCCP-FD	70.8	172.0	16.3	-	-	398.7	352.0	46.7	9.7
NRA	66.3	162.3	36.2	95.0	11.7	406.2	350.8	55.4	0.2
JRA	75.6	174.9	16.2	108.5	16.6	405.0	337.3	67.7	-17.9
HOAPS	-	-	-	103.6	14.6	-	-	56.1	-
WHOI	-	-	-	93.8	10.8	-	-		
This paper	78.2	167.8	16.6	97.1	12	400.7	343.3	57.4	1.3



view of the energy imbalance at the surface and the above discussion, we somewhat arbitrarily increase the GPCP values by 5%, in order to accommodate likely revisions from CloudSat studies and to bring them closer to CMAP in the tropics and subtropics. Hence, the global value assigned is  $80.0 \text{ W m}^{-2}$  ( $2.76 \text{ mm day}^{-1}$ ).

We apportion the latent heat flux values between ocean and land as in Trenberth et al. (2007a) by assuming a runoff into the ocean of  $40 \times 10^3 \text{ km}^3 \text{ yr}^{-1}$  (Trenberth et al. 2007a). The raw values based on GPCP over ocean of  $91.9 \text{ W m}^{-2}$  are reasonably close to (within 2%), but are a bit less than estimates of latent heat flux from WHOI ( $93.8 \text{ W m}^{-2}$ ). However, we impose the 5% global increase in precipitation only over the ocean, leaving the land precipitation unchanged from GPCP at  $2.06 \text{ mm day}^{-1}$ , while the ocean precipitation increases to  $3.06 \text{ mm day}^{-1}$ . ERA-40 precipitation values are known to be high and there is a global excess of model precipitation over evaporation (Uppala et al. 2005). JRA values are the highest over the ocean and JRA latent energy associated with global evaporation exceeds that of precipitation by an unrealistic  $3.2 \text{ W m}^{-2}$  for the CERES period.

The SH is available from the reanalyses for all years, and ranges from  $15.7$  and  $18.9 \text{ W m}^{-2}$  globally, from  $26.3$  to  $27.5 \text{ W m}^{-2}$  over land, and from  $11.8$  to  $16.0 \text{ W m}^{-2}$  over the ocean. The value in KT97 was computed as a residual and was unrealistically high at  $24 \text{ W m}^{-2}$ . Here we adopt values of  $17$ ,  $27$ , and  $12 \text{ W m}^{-2}$  for the globe, land, and ocean, and even with uncertainties of 10%, the errors are only order  $2 \text{ W m}^{-2}$ .

There is widespread agreement among the other estimates that the global mean surface upward LW radiation is about  $6 \text{ W m}^{-2}$  higher than the values in KT97 owing to the rectification effects described in the “Spatial and temporal sampling” sidebar. We adopt a value of  $396 \text{ W m}^{-2}$ , which is within  $2.1 \text{ W m}^{-2}$  of all estimates but is dependent on the skin temperature and surface emissivity (Zhang et al. 2006) and can not be pinned down more accurately. To compute the land and ocean contributions, we use the ISCCP-FD ratios.

This leaves the downward and net LW radiation as the final quantities to be computed as a residual. Our first attempt at this left a downward LW radiation much lower than most other estimates both for this and the ERBE period, as well as times in between. In particular it was  $24 \text{ W m}^{-2}$  lower than the ISCCP-FD value. This problem is illustrated in Table 2b when the HOAPS surface turbulent fluxes are combined

with ISCCP-FD radiation values, because there is a net over the ocean of  $9.7 \text{ W m}^{-2}$ , which includes a HOAPS high bias for LH of  $12 \text{ W m}^{-2}$ .

However, after the adjustments noted above for LH and better accounting for the aerosols and water vapor in the absorbed solar radiation, our revision estimates are  $333$  and  $63 \text{ W m}^{-2}$  for the downward and net LW. The latter is somewhat closer to and within the errors assessed for the ISCCP-FD value. The global annual mean Gupta et al. (1999) values for the surface radiation budget are similar to but with slightly larger discrepancies than for ISCCP-FD; their net LW is  $47.9 \text{ W m}^{-2}$ . Several other estimates of downward LW radiation are in the vicinity of  $340 \text{ W m}^{-2}$  (e.g., see ERA-40 in Table 1b) and Wild et al. (2001) have proposed that  $344 \text{ W m}^{-2}$  is a best estimate. These and other calculations are improved when performed with validated RRTM LW radiation codes (Wild and Roeckner 2006). However, Wild et al. (2001) note that considerable uncertainties exist, and especially that there were problems in accurate simulation of thermal emission from a cold, dry, cloud-free atmosphere, and a dependence on water vapor content. The latter may relate to the formulation of the water vapor continuum.

It has been argued that downward LW radiation is more likely to be underestimated owing to the view from satellites, which will miss underlying low clouds and make the cloud base too high. Wild and Roeckner (2006) have argued that the longwave fluxes should typically be rather higher than lower in climate models, which, in turn, are higher than the best estimate given here. Nevertheless, as they discuss, uncertainties are substantial. Zhang et al. (2006) found that the surface LW flux was very sensitive to assumptions about tropospheric water vapor and temperatures, but did not analyze the dependence on clouds. However, the characteristics of clouds on which the back radiation is most dependent, such as cloud base, are not well determined from space-based measurements (Gupta et al. 1999), and hence there is the need for missions such as CloudSat (e.g., Stephens et al. 2002; Haynes and Stephens 2007). There are also sources of error in how cloud overlap is treated and there is no unique way to treat the effects of overlap on the downward flux, which introduces uncertainties. For mid- and upper-level clouds, the cloud emissivity assumptions will also affect the estimated downward flux. Another source of error is the amount of water vapor between the surface and the cloud base. In the tropics, the effect of continuum absorption strongly affects the impact of cloud emission on surface long-wave fluxes.

In Table 2, most values are given to the first decimal place because this is necessary to resolve the NET, even though the values are not accurate to that level. Hence, most quantities when converted into Fig. 1 values are appropriately rounded.

**DISCUSSION.** In the above we have outlined the main issues and sources of problems in determining the energy budgets for Earth. It is desirable to examine the land and ocean domains separately to capitalize on the constraints that come with them related especially to the ability of the two domains to store energy at the surface. In Fasullo and Trenberth (2008a), we determined a best value for the CERES period of  $2.2 \pm 0.1$  PW transport of energy from ocean to land based on TOA measurements plus changes in energy storage in the atmosphere. The reanalyses had values grouped around this value but discrepancies, especially in their time series, relate to changes in the observing system and how those inhomogeneities affected the different reanalyses.

The annual mean transport of energy from the ocean to land occurs mainly in the northern winter where values are about 5 PW as stored energy emerges from the ocean and is transported over land where it can radiate to space (Fasullo and Trenberth 2008a,b). However, Trenberth et al. (2007a) show that the net transport of moisture from ocean to land as part of the hydrological cycle is equivalent to 3.2 PW of energy for the annual mean. Hence the net dry static energy transport is actually from land to ocean. This is clearly what happens in monsoons, for instance, where warm land and lower surface pressures bring onshore moisture-laden winds that produce monsoon rains and latent heat release while cooling the land and reducing ocean–land temperature and pressure gradients. In general, the vertically integrated latent energy and dry static energy transports are opposite in sign in monsoon and Hadley and Walker circulations throughout the lower latitudes (Trenberth and Stepaniak 2003a,b) and this influences the global budgets.

It is not possible to give very useful error bars to the estimates. Fasullo and Trenberth (2008a) provide error bars for the TOA radiation quantities, but they are based on temporal and spatial sampling issues, and more fundamental errors associated with instrumentation, calibration, modeling, and so on, can only be assessed in the qualitative manner we have done here, namely, by providing multiple estimates with some sense of their strengths and weaknesses. Loeb et al. (2009) provide further determinations of both the estimates given here and the sources of errors. In most cases we can readily say that particular estimates

are certainly not correct. Examples include the NRA excessive surface ocean albedo that caused large biases in surface reflection and absorption, known problems with cloud distributions in the reanalyses, and situations such as in the reanalyses where the TOA imbalance suggests biases and problems. Hence, we can often dismiss outliers. Thus, while the spread of the various values provides some measure of agreement, it generally greatly overestimates the uncertainty we can assign to our best estimates. Therefore, we have a lot more confidence in the values we have assigned than indicated by the spread within the tables. TOA values are known within about  $\pm 3\%$  or better, except that the net is (or was)  $0.85 \pm 0.15 \text{ W m}^{-2}$  (Hansen et al. 2005), and surface fluxes are constrained within 5% except for solar-reflected, LH, and LW, where errors may be as much as 10%.

We have attempted to put together energy budgets for the ERBE and CERES periods. Some differences arise from real changes in the climate such as changes in albedo from reduced snow and ice cover, as well as changes in atmospheric circulation and clouds (Trenberth et al. 2007b). However, changes in albedo are larger than can be accounted for in this way and arise from the improved CERES instruments and processing (Wielicki et al. 2006; Fasullo and Trenberth 2008a, Loeb et al. 2009). Increases in surface evaporation appear to be real (Yu and Weller 2007). Improvements in modeling have led to changes in other values, especially with the ISCCP-FD processing using realistic clouds, but also highlight that simulation of clouds in models used for reanalysis remains a major issue. Recent improvements in aerosol and water vapor absorption in the atmosphere have also been incorporated here.

Although the GPCP estimates of global precipitation are regarded as the best available, it is suspected that they may be biased low in the light of new CloudSat measurements, and we have allowed for this in an ad hoc way. Our resulting ocean LH values are within 3.5% of the best calibrated surface flux product from WHOI. The ERA-40 and JRA models overestimate surface evaporation and the hydrological cycle. In our analysis, the biggest uncertainty and bias comes from the downward longwave radiation. This source of uncertainty is likely mainly from clouds.

Accordingly, as well as providing our best estimate of the Earth's energy budget (Fig. 1) we have provided a discussion of problems and issues that can hopefully be addressed in the future.

**ACKNOWLEDGMENTS.** This research is partially sponsored by the NOAA CLIVAR and CCDD programs

under Grants NA06OAR4310145 and NA07OAR4310051. CERES data were obtained from the NASA Langley Distributed Data Archive. We thank Bruce Wielicki and

other members of the CERES team for their thoughtful comments and discussions. Thanks also to Martin Wild and Mike Bosilovich for comments.

## APPENDIX: ACRONYMS.

ASR	Absorbed solar radiation
CCM	Community Climate Model
CERES	Clouds and the Earth's Radiant Energy System
CLM:	Community Land Model
CMAP	NOAA Climate Prediction Center (CPC) Merged Analysis of Precipitation
ERBE	Earth Radiation Budget Experiment
ERBS	Earth Radiation Budget Satellite
ECMWF	European Centre for Medium Range Weather Forecasts
ENSO	El Niño–Southern Oscillation
ERA-40	40-yr ECWMF Re-Analysis
FM1, FM2	CERES twin instruments Flight Models 1 and 2 on the <i>Terra</i> spacecraft
GPCP	Global Precipitation Climatology Project
HOAPS	Hamburg Ocean Atmosphere Parameters and Fluxes from Satellite Data
ISCCP	International Satellite Cloud Climatology Project
JRA	Japanese reanalysis
LH	Latent heat
LW	Longwave
MODIS	Moderate Resolution Imaging Spectroradiometer
NCEP	National Center for Environmental Prediction
NCAR	National Centers for Atmospheric Research
NOAA	National Oceanic and Atmospheric Administration
NRA	NCEP–NCAR reanalysis
OLR	Outgoing longwave radiation
PW	Petawatt
RRTM	Rapid radiative transfer model
SH	Sensible heat
SOC	Southampton Oceanographic Centre
SRBAVG	Surface radiation budget average
TIM	Total irradiance monitor
TOA	Top of atmosphere
VOS	Voluntary observing ship
WHOI	Woods Hole Oceanographic Institution

## REFERENCES

- Adler, R. F., and Coauthors, 2003: The version 2 Global Precipitation Climatology Project (GPCP) monthly precipitation analysis (1979–present). *J. Hydrometeor.*, **4**, 1147–1167.
- Bentamy, A., K. B. Katsaros, A. M. Mestas-Núñez, W. M. Drennan, E. B. Forde, and H. Roquet, 2003: Satellite estimates of wind speed and latent heat flux over the global oceans. *J. Climate*, **16**, 637–656.
- Bony, S., Y. Sud, K. M. Lau, J. Susskind, and S. Saha, 1997: Comparison and satellite assessment of NASA/DOA and NCEP–NCAR reanalyses over tropical ocean: Atmospheric hydrology and radiation. *J. Climate*, **10**, 1441–1462.
- Cess, R. D., and Coauthors, 1995: Absorption of solar radiation by clouds: Observations versus models. *Science*, **267**, 496–499.
- Chédin, A., E. Péquignot, S. Serrar, and N. A. Scott, 2004: Simultaneous determination of continental surface emissivity and temperature from NOAA 10/HIRS observations: Analysis of their seasonal variations. *J. Geophys. Res.*, **109**, D20110, doi: 10.1029/2004JD004886.
- Dai, A., and K. E. Trenberth, 2002: Estimates of freshwater discharge from continents: Latitudinal and seasonal variations. *J. Hydrometeor.*, **3**, 660–687.
- , T. R. Karl, B. Sun, and K. E. Trenberth, 2006: Recent trends in cloudiness over the United States: A

- tale of monitoring inadequacies. *Bull. Amer. Meteor. Soc.*, **87**, 597–606.
- Fasullo, J. T., and K. E. Trenberth, 2008a: The annual cycle of the energy budget. Part I: Global mean and land–ocean exchanges. *J. Climate*, **21**, 2297–2313.
- , and —, 2008b: The annual cycle of the energy budget. Part II: Meridional structures and poleward transports. *J. Climate*, **21**, 2314–2326.
- Grist, J. P., and S. A. Josey, 2003: Inverse analysis of the SOC air–sea flux climatology using ocean heat transport constraints. *J. Climate*, **16**, 3274–3295.
- Gupta, S. K., N. A. Ritchey, A. C. Wilber, C. H. Whitlock, G. G. Gibson, and P. W. Stackhouse, 1999: A climatology of surface radiation budget derived from satellite data. *J. Climate*, **12**, 2691–2710.
- Hansen, J., and Coauthors, 2005: Earth’s energy imbalance: Confirmation and implications. *Science*, **308**, 1431–1435.
- Haynes, J. M., and G. L. Stephens, 2007: Tropical oceanic cloudiness and the incidence of precipitation: Early results from CloudSat. *Geophys. Res. Lett.*, **34**, L09811, doi:10.1029/2007GL029335.
- Huang, S., 2006: Land warming as part of global warming. *Eos, Trans. Amer. Geophys. Union*, **87**, 44.
- Jones, D., M. New, D. E. Parker, S. Martin, and I. G. Rigor, 1999: Surface air temperature and its changes over the past 150 years. *Rev. Geophys.*, **37**, 173–199.
- Kalnay, E., and Coauthors, 1996: The NCEP/NCAR 40-Year Reanalysis Project. *Bull. Amer. Meteor. Soc.*, **77**, 437–471.
- Kiehl, J. T., and K. E. Trenberth, 1997: Earth’s annual global mean energy budget. *Bull. Amer. Meteor. Soc.*, **78**, 197–208.
- Kim, D., and V. Ramanathan, 2008: Solar radiation and radiative forcing due to aerosols and clouds. *J. Geophys. Res.*, **113**, D02203, doi:10.1029/2007JD008434.
- Kopp, G., G. Lawrence, and G. Rottman, 2005: The Total Irradiance Monitor (TIM): Science results. *Solar Phys.*, **230**, 129–140.
- Levitus, S., J. Antonov, and T. Boyer, 2005: Warming of the world ocean, 1955–2003. *Geophys. Res. Lett.*, **32**, L02604, doi:10.1029/2004GL021592.
- Loeb, N. G., F. Parol, J. C. Buriez, and C. Vanbaue, 2000: Top-of-atmosphere albedo estimation from angular distribution models using scene identification from satellite cloud property retrievals. *J. Climate*, **13**, 1269–1285.
- , and Coauthors, 2007: Multi-instrument comparison of top-of-atmosphere reflected solar radiation. *J. Climate*, **20**, 575–591.
- , and Coauthors, 2009: Toward optimal closure of the Earth’s top-of-atmosphere radiation budget. *J. Climate*, in press.
- Onogi, K., and Coauthors, 2007: The JRA-25 reanalysis. *J. Meteor. Soc. Japan*, **85**, 369–432.
- Oreopoulos, L., A. Marshak, and R. F. Cahalan, 2003: Consistency of ARESE II cloud absorption estimates and sampling issues. *J. Geophys. Res.*, **108**, 4029, doi:10.1029/2002JD002243.
- Pilewskie, P., and F. P. J. Valero, 1995: Direct observations of excess solar absorption by clouds. *Science*, **267**, 1626–1629.
- Qian, T., A. Dai, K. E. Trenberth, and K. W. Oleson, 2006: Simulation of global land surface conditions from 1948–2004. Part I: Forcing data and evaluation. *J. Hydrometeor.*, **7**, 953–975.
- Ramanathan, V., B. Subasilar, G. J. Zhang, W. Conant, R. D. Cess, J. T. Kiehl, H. Grassl, and L. Shi, 1995: Warm pool heat budget and shortwave cloud forcing: A missing physics? *Science*, **267**, 499–503.
- , P. J. Crutzen, J. T. Kiehl, and D. Rosenfeld, 2001: Aerosols, climate, and the hydrological cycle. *Science*, **294**, 2119–2124.
- Rossow, W. B., and E. Duenas, 2004: The international satellite cloud climatology project (ISCCP) web site: An online resource for research. *Bull. Amer. Meteor. Soc.*, **85**, 167–172.
- Schlosser, C. A., and P. R. Houser, 2007: Assessing a satellite-era perspective of the global water cycle. *J. Climate*, **20**, 1316–1338.
- Smith, G. L., A. C. Wilber, S. K. Gupta, and P. W. Stackhouse, 2002: Surface radiation budget and climate classification. *J. Climate*, **15**, 1175–1188.
- Stephens, G. L., and S.-C. Tsay, 1990: On the cloud absorption anomaly. *Quart. J. Roy. Meteor. Soc.*, **116**, 671–704.
- , and J. M. Haynes, 2007: Near global observations of the warm rain coalescence process. *Geophys. Res. Lett.*, **34**, L20805, doi:10.1029/2007GL030259.
- , and Coauthors, 2002: The CloudSat mission and the A-Train. *Bull. Amer. Meteor. Soc.*, **83**, 1771–1790.
- Trenberth, K. E., 1997: Using atmospheric budgets as a constraint on surface fluxes. *J. Climate*, **10**, 2796–2809.
- , and J. M. Caron, 2001: Estimates of meridional atmosphere and ocean heat transports. *J. Climate*, **14**, 3433–3443.
- , and D. P. Stepaniak, 2003a: Covariability of components of poleward atmospheric energy transports on seasonal and interannual time scales. *J. Climate*, **16**, 3690–3704.
- , and —, 2003b: Seamless poleward atmospheric energy transports and implications for the Hadley circulation. *J. Climate*, **16**, 3705–3721.
- , and —, 2004: The flow of energy through the Earth’s climate system. *Quart. J. Roy. Meteor. Soc.*, **130**, 2677–2701.



- , and J. Fasullo, 2008: An observational estimate of ocean energy divergence. *J. Phys. Oceanogr.*, **38**, 984–999.
- , and L. Smith, 2008a: The three dimensional structure of the atmospheric energy budget: Methodology and evaluation. *Climate Dyn.*, in press, doi:10.1071/s00382-008-0389-3.
- , and —, 2008b: Atmospheric energy budgets in the Japanese Reanalysis: Evaluation and variability. *J. Meteor. Soc. Japan*, **86**, 579–592.
- , J. M. Caron, and D. P. Stepaniak, 2001: The atmospheric energy budget and implications for surface fluxes and ocean heat transports. *Climate Dyn.*, **17**, 259–276.
- , D. P. Stepaniak, and J. M. Caron, 2002: Interannual variations in the atmospheric heat budget. *J. Geophys. Res.*, **107**, 4066, 10.1029/2000JD000297.
- , J. Fasullo, and L. Smith, 2005: Trends and variability in column-integrated water vapor. *Climate Dyn.*, **24**, 741–758.
- , L. Smith, T. Qian, A. Dai, and J. Fasullo, 2007a: Estimates of the global water budget and its annual cycle using observational and model data. *J. Hydrometeor.*, **8**, 758–769.
- , and Coauthors, 2007b: Observations: Surface and atmospheric climate change. *Climate Change 2007: The Physical Science Basis*, S. Solomon et al., Eds., Cambridge University Press, 235–336.
- Uppala, S. M., and Coauthors, 2005: The ERA-40 reanalysis. *Quart. J. Roy. Meteor. Soc.*, **131**, 2961–3012.
- Weare, B. C., 1997: Comparison of NCEP–NCAR cloud radiative forcing reanalyses with observations. *J. Climate*, **10**, 2200–2209.
- Wielicki, B. A., B. R. Barkstrom, E. F. Harrison, R. B. Lee, G. L. Smith, and J. E. Cooper, 1996: Clouds and the earth’s radiant energy system (CERES): An earth observing system experiment. *Bull. Amer. Meteor. Soc.*, **77**, 853–868.
- , K. Priestley, P. Minnis, N. Loeb, D. Kratz, T. Charlock, D. Doelling, and D. Young, 2006: CERES radiation budget accuracy overview. Preprints, *12th Conf. Atmospheric Radiation*, Madison, WI, Amer. Meteor. Soc., 9.1.
- Wilber, A. C., D. P. Kratz, and S. K. Gupta, 1999: Surface emissivity maps for use in satellite retrievals of longwave radiation. NASA Tech. Publication NASA/TP-1999-209362, 35 pp.
- , G. L. Smith, S. K. Gupta, and P. W. Stackhouse, 2006: Annual cycles of surface shortwave radiative fluxes. *J. Climate*, **19**, 535–547.
- Wild, M., and E. Roeckner, 2006: Radiative fluxes in ECHAM5. *J. Climate*, **19**, 3792–3809.
- , A. Ohmura, H. Gilgen, J. J. Morecrette, and A. Slingo, 2001: Evaluation of downward longwave radiation in general circulation models. *J. Climate*, **14**, 3227–3239.
- , C. N. Long, and A. Ohmura, 2006: Evaluation of clear-sky solar fluxes in GCMs participating in AMIP and IPCC-AR4 from a surface perspective. *J. Geophys. Res.*, **111**, D01104, doi:10.1029/2005JD006118.
- Willis, J. K., D. Roemmich, and B. Cornuelle, 2004: Interannual variability in upper-ocean heat content, temperature, and thermosteric expansion on global scales. *J. Geophys. Res.*, **109**, C12036, doi:10.1029/2003JC002260.
- Wong, T., B. A. Wielicki, R. B. Lee, G. L. Smith, and K. Bush, 2006: Re-examination of the observed decadal variability of Earth Radiation Budget using altitude-corrected ERBE/ERBS nonscanner WFOV data. *J. Climate*, **19**, 4028–4040.
- Xie, P., and P. A. Arkin, 1997: Global precipitation: A 17-year monthly analysis based on gauge observations, satellite estimates and numerical model outputs. *Bull. Amer. Meteor. Soc.*, **78**, 2539–2558.
- Yin, X., A. Gruber, and P. Arkin, 2004: Comparison of the GPCP and CMAP merged gauge–satellite monthly precipitation products for the period 1979–2001. *J. Hydrometeor.*, **5**, 1207–1222.
- Yu, L. S., and R. A. Weller, 2007: Objectively analyzed air-sea heat fluxes for the global ice-free oceans (1981–2005). *Bull. Amer. Meteor. Soc.*, **88**, 527–539.
- , R. A. Weller, and B. Sun, 2004: Improving latent and sensible heat flux estimates for the Atlantic Ocean (1988–99) by a synthesis approach. *J. Climate*, **17**, 373–393.
- Zhang, Y.-C., and W. B. Rossow, 1997: Estimating meridional energy transports by the atmospheric and oceanic general circulations using boundary fluxes. *J. Climate*, **10**, 2358–2373.
- , —, A. A. Lacis, V. Oinas, and M. I. Mishchenko, 2004: Calculation of radiative fluxes from the surface to top of atmosphere based on ISCCP and other global data sets: Refinements of the radiative transfer model and the input data. *J. Geophys. Res.*, **109**, D19105, doi:10.1029/2003JD004457.
- , —, and P. W. Stackhouse Jr., 2006: Comparison of different global information sources used in surface radiative flux calculation: Radiative properties of the near-surface atmosphere. *J. Geophys. Res.*, **111**, D13106, doi:10.1029/2005JD006873.
- , —, —, A. Romanou, and B. A. Wielicki, 2007: Decadal variations of global energy and ocean heat budget and meridional energy transports inferred from recent global data sets. *J. Geophys. Res.*, **112**, D22101, doi:10.1029/2007JD0068435.